

## 3.3 FIELD GAMMA-RAY SPECTROMETRY

Contact Person(s) : Kevin M. Miller

### 3.3.1 SCOPE

This section describes the instrumentation, setup, calibration and analysis for EML's field (*in situ*)  $\gamma$ -ray spectrometry using high resolution Ge detectors. The specific application to inventory measurements is described, as well as a spectral stripping routine for total exposure rate measurements. Methods for low resolution NaI detectors are also given.

Field spectrometry is used at EML for the rapid identification of radionuclides in the environment. When the source geometry is taken into account, the concentrations or inventories (activity per unit area) of these radionuclides in the soil can be inferred along with the contribution to the above ground exposure rate. Applications have included:

1. the measurement of natural background and weapons test fallout emitters (Lowder et al., 1964a, b; Beck, 1966; Beck et al., 1964);
2. indoor radiation studies (Miller and Beck, 1984);
3. analysis of power reactor plumes (Gogolak, 1984);
4. the determination of aged fallout levels in terrain with mixed ground cover (Miller and Helfer, 1985).
5. site characterization for environmental restoration (Miller et al., 1994).

### 3.3.2 INSTRUMENTATION

Although field spectrometry can be performed with a NaI scintillator, the detector of choice at EML for most applications is a high resolution hyperpure germanium coaxial crystal. This type of detector can sustain warmup when not in use, which is a convenient feature during extended field trips.

Ease of handling is best accomplished with a detector mounted in a cryostat that is small (hand-held) and which has an all-attitude capability. Ideally, the detector assembly should be mounted on a tripod with the crystal endcap facing down toward the ground and the dewar above. This orientation maximizes the flux that will be intercepted and registered by the detector. However, a standard 17- or 30-L dewar with an upward facing endcap can still be used without a large loss in efficiency, since most of the flux is incident at the sidewall of the detector, with the dewar blocking out only a few percent of the ground area that is effectively being measured. In either the downward or upward facing geometries, the axis of rotation for the cylindrical crystal is perpendicular to the ground plane. As such, the detector can be assumed to have a symmetrical azimuthal response. A "goose neck" cryostat, where the crystal axis is parallel to the ground plane, should be avoided since this introduces asymmetry and would require making complicated angular corrections.

Counting times in the field can be reduced by using large volume detectors, however, the crystal length/diameter ratio is an important consideration as well. The standard method of measuring the efficiency for a Ge detector is performed with a  $^{60}\text{Co}$  source at 25 cm normal to the detector face. As mentioned above, the open field source geometry is such that most of the flux is incident from the side. Thus, for two detectors that have the same quoted efficiency, a long thin crystal will yield a higher count rate in the field as compared to a short wide one. However, length/diameter ratios close to unity would generally result in less uncertainty in measurements due to flatter angular responses.

A list of detectors that we have calibrated for field spectrometry is given in Table 3.1. Our current primary detector for field work is the 45% efficient high purity P-type Ge coaxial mounted in a portable (hand-held) cryostat. It requires a 6 h cool-down time before becoming operational, although it is normally mated to an overhead 30-L liquid nitrogen dewar with a gravity feed system when stored in the laboratory so that it is always ready for use. This type of setup also allows the detector to be placed in a shield and used for sample analysis. Once cooled down and detached from the feeder

dewar, the hand-held cryostat (1.2 L) can be used for as long as 24 h before refilling is required. For studies involving low energy, a recently acquired detector measures 75% in relative efficiency and is of N-type Ge with a beryllium window. It has a 3-L dewar and can be hand-held although it is best suited for tripod mounting.

Generally, measurements are made in the field using a portable battery-powered computer-based spectroscopy system. High voltage and preamplifier power are supplied to the detector by the system. Some detectors feature low power preamplifiers which provide for extended operational time when using battery power in the field. A spectroscopy grade amplifier is also contained within the system. The complete spectrometer system can be carried and operated by one person.

### 3.3.3 SITE SELECTION AND INSTRUMENT SETUP

The detector is placed ~1 m above the ground with the analyzer and operator positioned a few meters away. The site chosen should be a flat, relatively even and an open area. Terrain that has obstructions such as boulders, large felled or standing trees, and any man-made structures should be avoided as these will block the  $\gamma$  flux from the underlying soil. Extreme ground roughness will result in anomalies since the soil surface area close to the detector is increased, while the surface contribution from large distances is reduced. For measurements of fallout radionuclides, the area must be undisturbed in that water and wind erosion as well as human activity, such as cultivating, would tend to upset the distribution of any deposited activity. Figure 3.4 shows an example of equipment placement at a typical field site.

When selecting a site for measurement, the source geometry must be taken into account. An unshielded detector, placed at 1 m above the ground, samples the photon flux from a volume of soil out to a radius on the order of 10 m and down to a depth of about 30 cm, depending upon the photon energy. Figure 3.5 shows a pictorial representation of the relative ground area contributions to the primary (uncollided) flux at a height of 1 m for a medium energy (662 keV) source with a typical exponential depth profile in the soil. This effective "field of view" varies, being somewhat larger (smaller) for higher (lower) energy sources. Also, activity that is closer to the soil surface will produce a wider field of view. In effect, a field spectrum samples an area of several hundred square meters, thus averaging out the local inhomogeneities in the distribution of

the radionuclides. The source being measured is essentially a giant soil sample and counting statistics for a given spectral absorption peak are obtained in a fraction of the time required for counting a small collected sample.

A good practice to follow is to make a series of short measurements in an area to ensure that there is approximate uniformity before collecting a longer spectrum and obtaining the desired counting statistics. When making measurements of natural background, or when the exposure rate is dominated by the man-made emitters under study, this check can be performed with an ionization chamber or a suitably sensitive survey ratemeter in that uniform exposure rate readings would imply a spatially invariant source distribution relative to the detector. If the particular radionuclides under study contribute just a small fraction to the total exposure rate, then the corresponding peak area count rates should be checked with the spectrometer to ensure uniformity.

### 3.3.4 CALIBRATION

A complete description of field  $\gamma$ -ray spectrometry can be found in Beck et al. (1972) and Miller and Shebell (1995). To summarize, the exposure rate in air above the ground is related to the absorption peak counting rate registered by the detector by

$$\frac{N_f}{I} = \frac{N_0}{\phi} \frac{N_f}{N_0} \frac{\phi}{I} \quad (1)$$

where

$N_0/\phi$  is the counting rate from a particular spectrum absorption peak due to a unit primary photon flux density of energy E incident on the detector along the detector axis (normal to the detector face).

$N_f/N_0$  is the correction required to account for detector angular response, and

$\phi/I$  is the primary photon flux density with an energy E at the detector resulting from the decay of a particular radionuclide per unit exposure rate at the

detector from all primary and scattered photons originating from this nuclide and any others present from its radioactive decay series.

The first two terms depend on the particular detector;  $\phi/I$  values depend only on the source composition and geometry and can be used for any spectrometer calibration.

In a like manner, the concentration or inventory of a particular nuclide is related to absorption peak counting rate by

$$\frac{N_f}{A} = \frac{N_0}{\phi} \frac{N_f}{N_0} \frac{\phi}{A} \quad (2)$$

where  $\phi/A$  is the total photon flux density at the detector location per unit concentration or inventory of the nuclide.

The three factors to compute  $N_f/I$  or  $N_f/A$  are discussed separately.

#### A. $N_0/\phi$ .

The response to unit flux at normal incidence is evaluated for a detector using various  $\gamma$ -ray point sources. A complete energy response curve from 40 keV to 3 MeV can be inferred with a set made up with the reasonably long lived isotopes  $^{152}\text{Eu}$ ,  $^{241}\text{Am}$ ,  $^{137}\text{Cs}$ ,  $^{60}\text{Co}$ , and  $^{228}\text{Th}$ . The measurement procedure is as follows:

1. Position the source at a distance of at least 1 m and at normal incidence to the detector face.
2. Calculate the uncollided flux density at the detector effective crystal center, which is obtained by dividing the  $\gamma$  emission rate by  $4 \pi r^2$ . The value of  $r$  is the distance from the source to the crystal effective center. This can be taken to be the geometric center for high energy ( $> 1$  MeV) rays and the crystal face for low energy ( $< 0.1$  MeV)  $\gamma$  rays. For the energy range between these two values, an estimate of average penetration distance can be made based on the absorption coefficient of the crystal. The  $\gamma$  flux density is also corrected for air and source holder attenuation.

3. Collect a spectrum and determine the full absorption peak count rate.
4. Collect a spectrum without the source present and subtract out from the previously measured count rate any contribution to the peak from background emitters.
5. Divide the corrected count rate by the flux density to determine  $N_o/\phi$ .
6. Perform this measurement at different energies with either simultaneous or separate runs.
7. Plot the values of  $N_o/\phi$  versus energy on a log-log scale and fit the data to a smooth curve. Figure 3.6 shows  $N_o/\phi$  as function of energy above 200 keV for the detectors listed in Table 3.1. In the energy range shown, the response can be fit to a straight line on a log-log plot to within  $\pm 3\%$ .

### B. $N_f/N_o$ .

The uncollided  $\gamma$ -ray flux for a soil half space source geometry is not limited to angles normal to the detector face. Therefore, the complete flux density response calibration must account for the fact that a cylindrical Ge crystal when oriented with the axis of symmetry perpendicular to the ground plane has a variable altitudinal (zenith-angle) response. The correction factor,  $N_f/N_o$ , is determined from point source calibrations as functions of energy and angle in the vertical plane and can be calculated from

$$\frac{N_f}{N_o} = \int_0^x \frac{\phi(\theta)}{\phi} \frac{N(\theta)}{N_o} d\theta \quad (3)$$

where

$\phi(\theta)/\phi$  is the fraction of the total primary flux at zenith angle  $\theta$  for a given source energy and geometry, and

$N(\theta)/N$  is the response of the detector at angle  $\theta$  for the same energy  $\gamma$  ray relative to the response at normal incidence.

The procedure for determining the values of  $N_f/N_o$  is as follows:

1. Measure the full absorption peak count rate (minus any background contribution to the peak) using a point source at a fixed distance of at least 1 m to the crystal at  $15^\circ$  intervals between incident angles of  $0^\circ$  (normal to detector face) and  $90^\circ$ .
2. Plot the relative response  $N(\theta)/N$  versus angle and fit the data to a smooth curve.
3. Evaluate Equation 3 numerically for at least three different source distributions in the soil (surface plane, 3 cm relaxation depth, and uniform). The angular flux distribution data can be found in Beck et al. (1972).
4. Repeat Steps 1-3 for several other energies and plot the resultant values of  $N_f/N_o$  versus energy. The data points can be fit to a smooth curve for each source depth distribution.

As noted before, a longer crystal would tend to yield a higher count rate in the field, meaning that the value of  $N_f/N_o$  would be  $> 1$ . For the source distributions generally encountered, more than 80% of the uncollided flux is incident between  $\theta = 30^\circ$ - $90^\circ$  ( $\theta$  measured from the detector axis normal to the ground interface). Uniformity of the zenith angular response in this range to within a few percent assures that the value of  $N_f/N_o$  will not vary significantly with changes in the distribution of flux. In general, a more uniform response is achieved with a crystal where the diameter is close to the length dimension. However, the variation in  $N_f/N_o$  for a detector where the crystal length/diameter is as high as 1.3 or as low as 0.7 would not be expected to be more than about 20% for energies  $>200$  keV. Figure 3.7 shows angular correction factor data at three different energies for several detectors in a downward facing geometry and a uniform source depth profile.

### C. $\phi/I$ and $\phi/A$ .

The  $\phi/I$  (and  $\phi/A$ ) factors are derived from  $\gamma$ -ray transport calculations. Tabulations of these data along with other pertinent information on the make-up of the environmental  $\gamma$  radiation field can be found in Beck et al. (1972), Beck and de Planque (1968), and Beck (1972). A complete set of exposure rate values ( $I/A$ ) for close to 200 common

fission and activation isotopes at various exponential depth distributions in the soil can be found in Beck (1980).

**Notes:**

1. The inference of exposure rates from nuclides located in the ground does not require a precise knowledge of the distribution with depth or of the exact soil density or composition. This property results because the observed peak count rate in a field spectrum is essentially a measure of the uncollided flux, and although this quantity and the exposure rate produced by it and the associated scattered flux varies significantly with the source depth distribution and soil characteristics, the ratio of these two quantities,  $\phi/I$ , does not. Thus, even a crude estimate of source distribution should not lead to a sizeable error in the exposure rate.
2. In lieu of a complete experimental calibration of a Ge detector for field spectrometry, generic factors may be substituted at energies  $> 200$  keV (Helfer and Miller, 1988). The only parameters needed to apply this semiempirical calibration method are the manufacturer's quoted efficiency at 1332 keV (5-45%), the crystal length/diameter ratio (0.5-1.3), and the detector orientation in the field (upward or downward facing). The accuracy of the derived factors is estimated to be  $\pm 10\%$  for energies  $> 500$  keV and  $\pm 15\%$  for energies between 200 and 500 keV.

### 3.3.5 SPECTRUM ANALYSIS

In many situations, the built-in peak area estimate features of state-of-the-art analyzers are used in providing quick results in the field. Prominent peaks are identified in a bench-mark spectrum and the appropriate regions of interest are set up. On certain analyzers, function keys are programmed using the net peak area, counting time and calibration factor ( $N_p/I$  and  $N_p/A$ ) to provide instantaneous readout of exposure rate and concentration or inventory.

For more complete data reduction, a small computer is interfaced to the analyzer to run a spectrum analysis program. If desired, a totally portable system may be configured using a battery-powered laptop computer. Our standard analysis program (Gogolak and Miller, 1977; Gogolak, 1982) performs the following:



1. Based on a two point energy calibration as set by the operator, certain peaks which are characteristic of typical environmental spectra are identified, namely:
  - a. the 186, 295, 352, 609, 1120 and 1765 keV peaks in the  $^{238}\text{U}$  series;
  - b. the 583, 911, 966 and 2615 keV peaks in the  $^{232}\text{Th}$  series;
  - c. the 1460 keV peak of  $^{40}\text{K}$ ;
  - d. the 662 keV peak of  $^{137}\text{Cs}$ .

These peaks are defined by set energy bands where the left and right channel markers are representative of the Compton continuum.

2. The counts between the energy boundaries for each of the above peaks are summed. The background counts in three channels on each side of a peak are averaged and the result is used as an estimate of the baseline under the peak. This is multiplied by the number of channels in the peak and subtracted out from the total counts in the peak band to yield the net peak counts.
3. Detector specific calibration factors are applied to convert from peak count rate to exposure rate and concentration or inventory.
4. A printout is made listing count rates, converted quantities and associated statistical counting errors.
5. Permanent storage of the spectrum is made on either magnetic tape or diskette.
6. As an option, an automated search is performed to identify any peaks present in the spectrum. Data such as nuclide, half-life,  $\gamma$ -ray intensity and associated energy are printed out using a library of nearly 400 principal  $\gamma$ -ray energies that are seen in the environment (Section 5, this Manual). Any peak can be quickly analyzed by using an optional automated continuum strip.
7. The program enters an interactive phase where the operator examines any additional peaks, checks the results of the automated routine, or investigates any unusual or unexpected features of a spectrum.

### 3.3.6 INVENTORY MEASUREMENTS

#### 3.3.6.1 APPLICATION

---

A field  $\gamma$ -ray spectrum can also provide an estimate of the amount of activity per unit area of soil surface for nuclides which have been deposited on the ground. To do this, a knowledge of the source distribution in the soil is required in order to relate the measured total absorption peak count rate to the incident unscattered photon flux and then to the activity in the soil in a manner analogous to that used for natural emitters.

The activity profile with depth for deposited nuclides in undisturbed soils can be represented by an exponential function,

$$S = S_0 e^{-(\alpha/\rho)\rho z} \quad (4)$$

where

- S is the activity per  $\text{cm}^3$  at depth  $z$  cm,
- $S_0$  is the activity per  $\text{cm}^3$  at the soil surface,
- $\alpha$  is the reciprocal of the relaxation length in  $\text{cm}^{-1}$ , and
- $\rho$  is the *in situ* soil density ( $\text{g cm}^{-2}$ ).

The cumulative activity, or inventory  $I$ , integrated to depth  $z'$  is, then,

$$I = \int_0^{z'} dz = \frac{S_0}{\alpha} \left[ 1 - e^{-(\alpha/\rho)\rho z'} \right] = I_0 \left[ 1 - e^{-(\alpha/\rho)\rho z'} \right] \quad (5)$$

where  $I_0$  is the total inventory integrated to infinite depth.

### 3.3.6.2 HOMOGENEOUS TERRAIN

---

In the case of a freshly deposited nuclide, the depth parameter is infinite corresponding to a plane source distribution and a relaxation length of zero. In practice, the effects of ground roughness bury the source somewhat. Even on what appears to be flat terrain, we apply an  $\alpha/\rho$  value of  $6.25 \text{ cm}^2 \text{ g}^{-1}$ , which at a typical soil density of  $1.6 \text{ g cm}^{-3}$  corresponds to a relaxation depth of 0.1 cm. Values of  $\alpha/\rho$  for aged global fallout  $^{137}\text{Cs}$  have been found to range from a high of 1.0 for an evergreen forest floor to a low of 0.03 for a flood irrigated lawn. At a soil density of  $1.6 \text{ g cm}^{-3}$ , these correspond to relaxation lengths of 0.6 and 21 cm, respectively. More typical values of  $\alpha/\rho$  tend to range from 0.05-0.1 for open field sites and 0.2-0.5 for wooded or desert areas.

Values of the unscattered flux and its angular distribution at 1 m above the ground have been tabulated for exponentially distributed sources in the soil for various energies and  $\alpha/\rho$  values (Beck et al., 1972). Using Equation 2, where the term A now represents the inventory (activity per unit area), the detector response can be calculated for a particular nuclide as a function of  $\alpha/\rho$ . If the nuclide has two reasonably strong  $\gamma$  lines well separated in energy, the value of  $\alpha/\rho$  can be inferred from the ratio of the measured fluxes.

In the case of a monoenergetic source such as  $^{137}\text{Cs}$ , the value of  $\alpha/\rho$  can be determined experimentally as follows:

1. A  $62 \text{ cm}^2$  or similar large area corer and auger is used to extract soil samples from different depth intervals (see Section 2.4) depending upon the expected activity distribution. For example, if the profile is expected to be shallow, the depth intervals can be 0-2.5, 2.5-5, and 5-30 cm, while if it is expected to be deep, intervals of 0-5 cm, 5-10 cm, and 10-30 cm can be used. More than one core can be taken, in which case the samples from the same depth are composited. The depth of the soil core should be sufficient to include essentially all of the deposited activity so that  $I_0$  can be determined.
2. An aliquot of a sample from each depth increment is counted on a high resolution Ge detector to determine the concentration of the radionuclide of interest.

3. The activity per unit area for each depth is computed from the product of the concentration and the sample mass for that depth increment divided by the area of the sample.
4. A fit to Equation 5 is then applied, the variables being  $I_0 - I$ , the integrated activity per unit area and  $\rho z'$ , the gross *in situ* mass per unit area down to depth  $z'$ . Graphically, this can be performed by plotting the  $\log(I_0 - I)$  versus  $\rho z$  and fitting a straight line through the points, weighting the points near the surface more heavily since this is where most of the activity is contained. The slope of this line is just  $\alpha/\rho$ .

**Note:**

Although the inventory is determined using the soil sample data itself, it is quite useful to corroborate this estimate with the field spectrum. The soil cores may represent an area of a few hundred square centimeters, while the field data represent the average over several hundred square meters.

3.3.6.3

**NONHOMOGENEOUS TERRAIN**

---

For areas where the fallout is suspected of being unevenly distributed across the ground, representative inventory measurements can still be made by relying on the fact that a field spectrum averages out the local inhomogeneities in the source geometry. This more generalized method is applied to cases such as the measurement of aged fallout in the desert southwest of the U.S. where blowsand tends to shift from bare soil and collect under vegetative cover. A complete description can be found in Miller and Helfer (1985). The basic steps include:

1. Soil samples in depth increments are collected from the different types of ground cover present (grass, brush, bare soil, etc.).
2. The samples are counted and a depth profile for each type of ground cover is obtained using the procedure outlined above for homogeneous terrain.

3. If the depth profiles are significantly different, the approximate percentage of ground cover of each type is determined within a 15 x 15 m square centered at the detector. This can be performed using a combination of tape measurements and eye estimates to approximate the dimensions of any patches of grass or shrubs and trees out to their drip line, or to where there is an obvious change in soil characteristics, and then calculating the total area of each particular type of cover.
4. The conversion factor to apply to the peak count rate in order to obtain an inventory estimate is given by

$$\langle g \rangle = \left[ \sum_i \frac{x_i}{g_i} \right]^{-1} \quad (6)$$

where

- $\langle g \rangle$  is the average full absorption peak count rate to inventory conversion factor for an infinite half space source distribution with randomly spaced segments of different types of ground cover, each of which has its own characteristic nuclide depth distribution and inventory (inventory per unit count rate),
- $x_i$  is the fraction of the total inventory associated with the i-th type of ground cover,
- $g_i$  is the full absorption peak count rate to inventory conversion factor for an infinite half-space source distribution with a measured depth profile characteristic of the i-th type of ground cover (inventory per unit count rate).

**Note:**

The value of  $\langle g \rangle$  exhibits a dependence on the relative inventory mix for the different ground covers which can only be determined through soil sampling. Nonetheless, the value of  $\langle g \rangle$  must fall within the range of the individual values of  $g_i$ . Generally, this range is not large. Although the inventory may typically vary by a factor of two for the different ground covers, the variation in the conversion factor for the different depth

profiles associated with these ground covers will average <30%. This is particularly true for sites where the fallout is near the soil surface because the conversion factor does not vary strongly with the depth profile for values of  $\alpha/\rho > 0.2$ .

### 3.3.7 SPECTRAL STRIPPING FOR GERMANIUM DETECTORS

#### 3.3.7.1 APPLICATION

---

A stripping operation can be applied to a Ge detector spectrum which has been collected in free air in order to obtain the  $\gamma$  flux density as a function of energy (Miller, 1984). This flux spectrum can be readily converted to an independent estimate of the free air exposure rate or be used to make energy response corrections to other radiation measuring devices. This technique has particular applications to indoor radiation measurements, where the flux distribution is not easily predicted because of the complex and generally unknown  $\gamma$  source geometry.

#### 3.3.7.2 THEORY

---

A count registered by the detector can be caused by the full or partial absorption of an incident photon or by the passage of a cosmic ray produced charged particle. In order to obtain a measure of the incident photon flux spectrum, the partial absorption and cosmic-ray events must be subtracted out and then the full absorption efficiency curve of the detector can be applied.

The stripping operation can be expressed as:

$$N_1' = N_1 - \sum_{j=1}^L f_{ij}(r_j - 1) N_j' - N_c \quad (7)$$

where

$N_i', N_j'$  are the counts in an energy band due to the total absorption of incident  $\gamma$  flux,  
 $N_i$  is the observed counts in an energy band due to all sources,  
 $L$  is the energy band containing the highest energy  $\gamma$  line (generally 2.615 keV),

$f_{ij}$  is the fraction of the continuum counts at energy band  $i$  due to the partial absorption of incident  $\gamma$  flux at energy band  $j$ ,

$r_j$  is the ratio of total counts to full absorption peak counts for incident flux at energy band  $j$ , and

$N_c$  is the counts in band  $i$  due to cosmic-ray events, assumed to be constant in any energy band and given by

$$N_c = (E_2 - E_1 + 1)^{-1} \sum_{i=E_1}^{E_2} N_i \quad (8)$$

where

$E_1, E_2$  are the lower and upper energy bands of a pure cosmic-ray energy (generally 3-4 MeV).

### 3.3.7.3

#### DETERMINATION OF STRIPPING PARAMETERS (f and r)

---

Factor f - For the factor  $f$ , a multiple step function fit is used wherein the region below the Compton edge is divided into 10 equal size energy bands and the region above the Compton edge is divided into four equal bands. The fraction of the total counts in the continuum in each band can be experimentally determined for a particular detector by examining the shape of the continuum below a full absorption peak from a mono-energetic  $\gamma$  source. Although the shape of the continuum is a function of the energy and

incident angle of the  $\gamma$  ray, it is not overly sensitive to these variables, particularly at the higher energies which contribute the most to the exposure rate.

Factor  $r$  - In the same manner that the full absorption peak efficiency is determined for a detector (see Procedure 3.3.4 for  $N_o/\phi$ ), the total efficiency can be determined and its ratio computed. However, effectively monoenergetic sources must be used and room background must be subtracted from the entire spectrum. Like the full absorption peak efficiency, the total efficiency varies with incident angle for a cylindrical detector. However, the ratio of the two,  $r$ , varies more smoothly and is not a strong function of the incident angle. A single angular correction factor can therefore be applied which is representative of the higher  $\gamma$  energies which weigh heavily in the exposure rate computation. This factor can be obtained by assuming an isotropic radiation field and averaging over the entire  $4\pi$  solid angle. Although, in practice, the radiation field may not be isotropic, a reasonable approximation to this ideal can be created by accumulating a spectrum with the detector oriented in different directions, thus averaging out the angular dependence. To accomplish this, we routinely count for equal lengths of time with the detector pointing in six different directions, that is, each way along three orthogonal axes.

#### 3.3.7.4

### STRIPPING OPERATION

---

The stripping operation is performed on a portable PC using Basic and takes < 1 min to complete. It proceeds as follows:

1. The spectrum is calibrated using two energy-channel points supplied by the operator.
2. The spectrum is compressed from 4000 channels to 400 channels for faster computation.
3. The spectrum is stripped of the cosmic-ray events.



4. The spectrum is stripped of partial absorption events for equal size energy bands of 10 keV each and starting at the band containing the highest energy  $\gamma$  line (generally 2.615 keV), where  $N' = N - N_c$ . Succeeding lower energy bands can then be computed based on the  $N_j'$  values from any higher band.
5. The spectrum of counts which remains after the stripping operation is completed is converted to the incident flux density energy distribution by applying the full absorption peak efficiency of the detector. As in the case of the factor  $r$ , an angular correction based on the assumption of isotropic incidence must be applied.
6. The  $\gamma$  exposure rate is computed by integrating across the spectrum the product of the energy, flux density, and mass energy absorption coefficient for air at each energy band.

**Note:**

Intercomparisons between the spectral stripping method and our own instruments and standard procedures, as well as with those of the Japanese Atomic Energy Research Institute, have shown good agreement (Nagaoka, 1987). Based on these measurements, we conservatively estimate an upper limit in the total systematic error of  $\pm 5\%$  when this method is applied to spectra at background levels. The statistical error was determined to be  $< \pm 2\%$  (at the  $1 \sigma$  level) for a 1-min spectrum at typical background levels.

### 3.3.8 SODIUM IODIDE DETECTORS

#### 3.3.8.1

#### APPLICATION

---

Although no longer used routinely by EML for field  $\gamma$ -ray spectrometry, NaI detectors are nonetheless capable of yielding satisfactory results particularly for natural background measurements. Like the case for Ge detector measurements, full absorption analysis can be applied to a NaI field spectrum. In addition, there is the technique of "energy band" analysis as well as "total spectrum energy" analysis. A complete description of these methods can be found in Beck et al. (1972).

### 3.3.8.2

#### **EQUIPMENT**

---

The NaI detectors (usually 4-x-4 in cylindrical crystals attached to matched photomultiplier tubes) are coupled through an emitter-follower preamplifier. Either a battery powered portable or 120 V AC vehicle-based analyzer with at least 400 channels is used to collect the spectra. NaI detectors are usually covered (in addition to the manufacturer's standard thin aluminum or stainless steel window) by a 6-mm bakelite shield to reduce the  $\beta$ -ray contribution to the Compton continuum as well as to moderate thermal stresses. The NaI detector is transported in a rugged, foam-cushioned box to minimize mechanical and thermal shock.

### 3.3.8.3

#### **PEAK ANALYSIS**

---

For NaI spectrometry, the  $N_o/\phi$  should be obtained with source energies as close as possible to those environmental sources to be evaluated, usually the energies associated with the  $^{238}\text{U}$  and  $^{232}\text{Th}$  series,  $^{40}\text{K}$ , and  $^{137}\text{Cs}$ . The resulting  $N_o/\phi$  versus E data do not represent the usual NaI response curve, because the analysis of absorption peaks does not lead to accurate estimates of the actual peak areas, unless one engages in a complex computer program for spectral stripping. NaI peak areas are determined in essentially the same manner as those from Ge detectors, though only a few absorption peaks are measurable due to the relatively poor resolution. Cross-calibration of a NaI detector with the more accurate Ge detector can be very helpful.

### 3.3.8.4

#### **ENERGY BAND ANALYSIS**

---

When the naturally-occurring nuclides associated with the  $^{238}\text{U}$  and  $^{232}\text{Th}$  series and  $^{40}\text{K}$  predominate at a field site, the simplified "energy band" method of analysis can be

applied. In this method, the spectrum energy is calculated as the product of the counts per channel times the energy represented by each channel in bands of channels. The energy bands are centered on the 1.46 MeV <sup>40</sup>K, the 1.76 MeV <sup>214</sup>Bi, and the 2.62 MeV <sup>208</sup>Tl peaks. The response in each bin can then be represented by the following equations.

$$\begin{aligned}
 E_1 &= u_1U + k_1K + t_1T + I_1 \\
 E_2 &= u_2U + k_2K + t_2T + I_2 \\
 E_3 &= t_3T + I_3
 \end{aligned}
 \tag{9}$$

where  $E_1$ ,  $E_2$  and  $E_3$  are the measured "energy" values for some arbitrary counting period; U, K and T represent the exposure rates to be measured; the constants represent the distribution of spectrum energy per unit exposure rate among the three energy bands; and  $I_1$ ,  $I_2$  and  $I_3$  are the cosmic-ray contributions. The three equations relating the U, K and T exposure rates to the energy bands are determined by solving Equation 9 and evaluating the coefficients from regression analyses of a large number of field spectra for which exposure rates had been determined from absorption peak analyses.

The following approximate equations apply for a nominal 10.16 x 10.16 cm NaI detector, shielded with 6-mm Bakelite, though calibration of individual detectors is preferred.

$$\begin{aligned}
 U &= 0.4 E_1' - 0.2 E_3' \\
 K &= 0.08 E_1' - 0.06 E_2' - 0.02 E_3' \\
 T &= 0.3 E_3'
 \end{aligned}
 \tag{10}$$

and

$$I = E_T' / 37$$

where I is the total exposure rate from natural radioactivity in soil, and

$$\begin{aligned}1.32 \text{ MeV} < E_1' < 1.60 \text{ MeV}, \\1.62 \text{ MeV} < E_2' < 1.90 \text{ MeV}, \\2.48 \text{ MeV} < E_3' < 2.75 \text{ MeV}, \\0.15 \text{ MeV} < E_T' < 3.40 \text{ MeV},\end{aligned}$$

the E values being in GeV per 20-min counting period. The primes indicate that the energy contributions from cosmic rays must be subtracted before Equations 10 are used.

Energy band analysis is performed quickly in the field by interfacing the multichannel analyzer to a portable computer. Using interactive software (Gogolak and Miller, 1977), the basic steps include:

1. The spectrum is read into the computer and the operator provides a two point energy calibration (usually the positions of the 1460 keV  $^{40}\text{K}$  and 2615 keV  $^{208}\text{Tl}$  peaks) and the altitude to the nearest thousand feet (for the cosmic-ray corrections).
2. The above equations are applied.
3. A printout is made of the total exposure rate and the contributions for  $^{40}\text{K}$  and the  $^{238}\text{U}$  and  $^{232}\text{Th}$  series.

#### 3.3.8.5

#### **TOTAL SPECTRUM ENERGY ANALYSIS**

---

The exposure rate in air is proportional to  $\int_0^\infty \phi(E) (\mu_e/\rho) E dE$ , where  $\phi(E)$  is the flux of  $\gamma$  rays of energy E and  $\mu_e/\rho$  is the mass absorption coefficient in air. Between a few hundred keV and several MeV,  $\mu_e/\rho$  is fairly constant. Also for low energies, the probability of an incident photon being totally absorbed by a large NaI detector is fairly high (on the order of 50-100% from 100 keV to 1 MeV). About 75% of the exposure rate from the soil is due to emitters between 100 keV and 1500 keV. This and the fact that the spectrum of  $\gamma$  rays from natural emitters is fairly invariant to the exact proportions of U, Th and K in the soil, indicates that the total "spectrum energy" is a reasonable measure

of free air exposure from natural radioactivity in the soil. A large NaI or similar detector measures the flux to a fairly high degree of accuracy and, even though sensitivity decreases somewhat at higher energies due to the escape of secondary scattered photons, this decrease tends to be compensated by correspondingly smaller values of  $\mu_e/\rho$  for energies above 1 MeV relative to values below 1 MeV.

Unlike many NaI hand-held survey instruments, which depend on the assumption that the counting rate above some bias level is proportional to the exposure rate, the total energy technique requires only that the counts in a channel be proportional to  $\phi(E)(\mu_e/\rho)$  for that energy, and is, therefore, less sensitive to spectral changes. For example, a NaI survey meter might indicate that the exposure rate from a unit flux of 60 keV photons as being almost equal to the exposure rate from a unit flux of 1460 keV photons. This would occur since the 1460 keV pulse would be recorded due to the high probability of a Compton collision in the detector even though many of the secondaries would escape the crystal. In the total energy technique, the higher energy counts are weighted by the energy deposited and reflect their relative contribution to the exposure rate more correctly. The slightly larger total absorption at 60 keV reflects the larger value of  $(\mu_e/\rho)$  relative to higher energy  $\gamma$  rays.

The spectrum "energy" calibration factors for 10.16 x 10.16 cm detectors are determined in two ways:

1. The detectors are exposed to a known point source of  $^{226}\text{Ra}$  in the laboratory and the measured exposure rate is compared to an ionization chamber reading. The measurement should be corrected to account for the fact that the rays from the point source are incident along the detector axis.
2. A comparison of measurements of "spectrum energy" from actual field spectra is made with simultaneous ionization chamber measurements for different environmental radiation fields.

The two methods give essentially the same calibration factors.

## REFERENCES

Beck, H. L.

"Environmental Gamma Radiation from Deposited Fission Products, 1960 - 1964"  
Health Physics, 12, 313-322 (1966)

Beck, H. L.

"The Physics of Environmental Gamma Radiation Fields"

J. A. S. Adams, W. M. Lowder, and T. F. Gesell (Editors)

In: *The Natural Radiation Environment II*, CONF-720805-P1, pp. 101-134 (1972)

Beck, H. L.

"Exposure Rate Conversion Factors for Radionuclides Deposited on the Ground"

USDOE Report EML-378, July (1980)

Beck, H. L. and G. de Planque

"The Radiation Field in Air Due to Distributed Gamma-Ray Sources in the Ground"

USAEC Report HASL-195, May (1968)

Beck, H. L., W. J. Condo and W. M. Lowder

"Spectrometric Techniques for Measuring Environmental Gamma Radiation"

USAEC Report HASL-150, October (1964)

Beck, H. L., J. A. De Campo and C. V. Gogolak

"In Situ Ge(Li) and NaI(Tl) Gamma-Ray Spectrometry for the Measurement of  
Environmental Radiation"

USAEC Report HASL-258, July (1972)

Gogolak, C. V.

"Collection and Analysis of Environmental Radiation Data Using a Portable Desktop  
Computer"

USDOE Report EML-398, April (1982)

Gogolak, C. V.

"Rapid Determinations of Noble Gas Radionuclide Concentrations in Power Reactor  
Plumes"

Health Physics, 46, 783-792 (1984)

Gogolak, C. V. and K. M. Miller

"New Developments in Field Gamma-Ray Spectrometry"

USDOE Report EML-332, December (1977)

Helfer, I. K. and K. M. Miller

"Calibration Factors for Germanium Detectors Used for Field Spectrometry"

Health Physics, 55, 15-29 (1988)

Lowder W. M., H. L. Beck, and W. J. Condo

"Spectrometric Determination of Dose Rates from Natural and Fall-Out  
Gamma-Radiation in the United States, 1962-63"

Nature, 202, 745 (1964a)

Lowder W. M., W. J. Condo and H. L. Beck

"Field Spectrometric Investigations of Environmental Radiation in the U.S.A."

In: *The Natural Radiation Environment*, University of Chicago Press, Chicago, IL,  
pp. 597-616 (1964b)

Miller, K. M.

"A Spectral Stripping Method for a Ge Spectrometer Used for Indoor Gamma  
Exposure Rate Measurements"

USDOE Report EML-419, July (1984)

Miller, K. M. and H. L. Beck

"Indoor Gamma and Cosmic Ray Exposure Measurements Using a Ge Spectrometer  
and Pressurized Ionisation Chamber"

Radiation Protection Dosimetry, 7, 185-189 (1984)

Miller, K. M. and I. K. Helfer

"*In Situ* Measurements of <sup>137</sup>Cs Inventory in Natural Terrain"

In: Environmental Radiation '85, Proceedings of the Eighteenth Midyear Topical  
Symposium of the Health Physics Society, pp. 243-251 (1985)

Miller, K. M. and P. Shebell

"*In Situ* Gamma-Ray Spectrometry - A Tutorial for Environmental Radiation Scientists"

USDOE Report EML-557, October (1995)

Miller, K. M., P. Shebell and G. A. Klemic

"*In Situ* Gamma-Ray Spectrometry for the Measurement of Uranium in Surface Soils"

Health Physics, 67, 140-150 (1994)

Nagaoka, T.

"Intercomparison Between EML Method and JAERI Method for the Measurement of  
Environmental Gamma Ray Exposure Rates"  
Radiation Protection Dosimetry, 18, 81-88 (1987)



Table 3.1  
 Ge DETECTOR SPECIFICATIONS

Manufacturer	Serial No.	Code	Type	Cryostat orientation	Efficiency (%)	Resolution at 1332 (keV)	Dimensions DxL (mm)	L/D <sup>†</sup>	Peak/Compton
*Princeton Gamma-tech	484	P1	Ge(Li)	4 L, downward	2.9	1.70	36 x 20	0.56	23.0
	514	P2	Ge(Li)	4 L, downward	12.2	2.43	43 x 44	1.02	30.0
	1039	P3	Ge(Li)	17 L, upward	27.9	2.36	59 x 47	0.80	35.9
	1545	P4	Ge(Li)	17 L, upward	22.3	2.10	56 x 54	0.96	49.5
	1030	P5	P-type Ge	2 L, all attitude	21.7	1.77	59 x 35	0.59	52.0
**EG & G Ortec	23-N-37VB	O1	N-type Ge	30 L, upward	35.3	1.96	55 x 65	1.18	59.4
	25-N-1514	O2	N-type Ge	30 L, upward	35.4	1.73	55 x 73	1.31	67.9
	26-P-70P	O3	P-type Ge	1.8 L, all attitude	45.0	1.80	60 x 79	1.31	73.0
	33-TN30860A	-	N-type Ge	3 L, all-attitude	75.0	1.95	71 x 79	1.11	74.8

\*Princeton Gamma-Tech, Inc., 1200 State Road, Princeton, NJ 08540

\*\*EG & G Ortec, 100 Midland Road, Oak Ridge, TN 37830

<sup>†</sup>Ge crystal length/diameter ratio



Figure 3.4. Typical field site for conducting *in situ*  $\gamma$ -ray spectrometry showing placement of tripod mounted portable Ge detector and battery-powered multichannel analyzer.

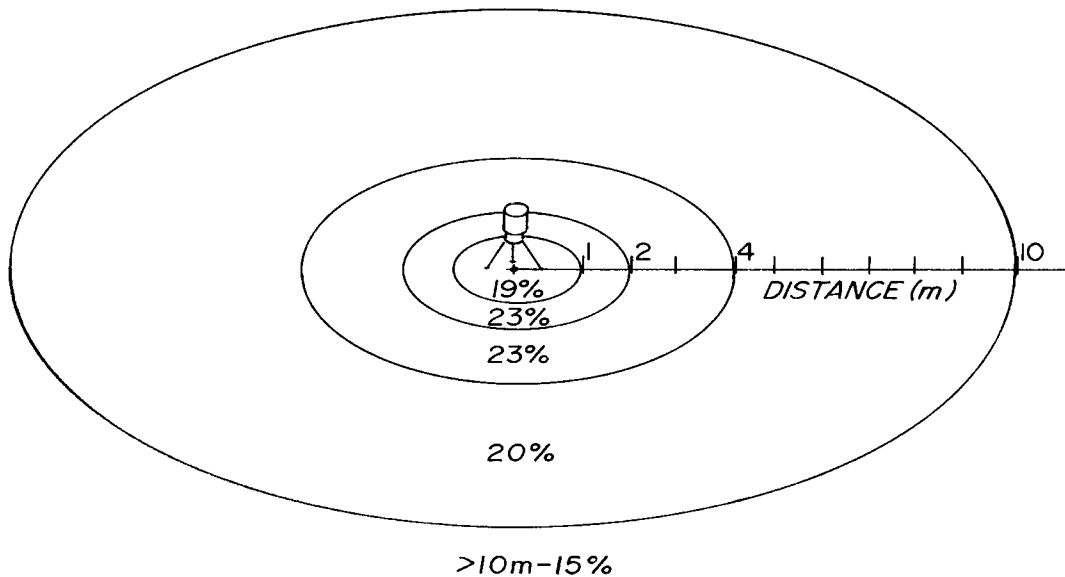


Figure 3.5. Schematic representation of the relative ground area contributions to the primary flux at 1 m above the ground for an exponentially distributed source with an energy of 662 keV and where  $\alpha/\rho = 0.21 \text{ cm}^2 \text{ g}^{-1}$ .

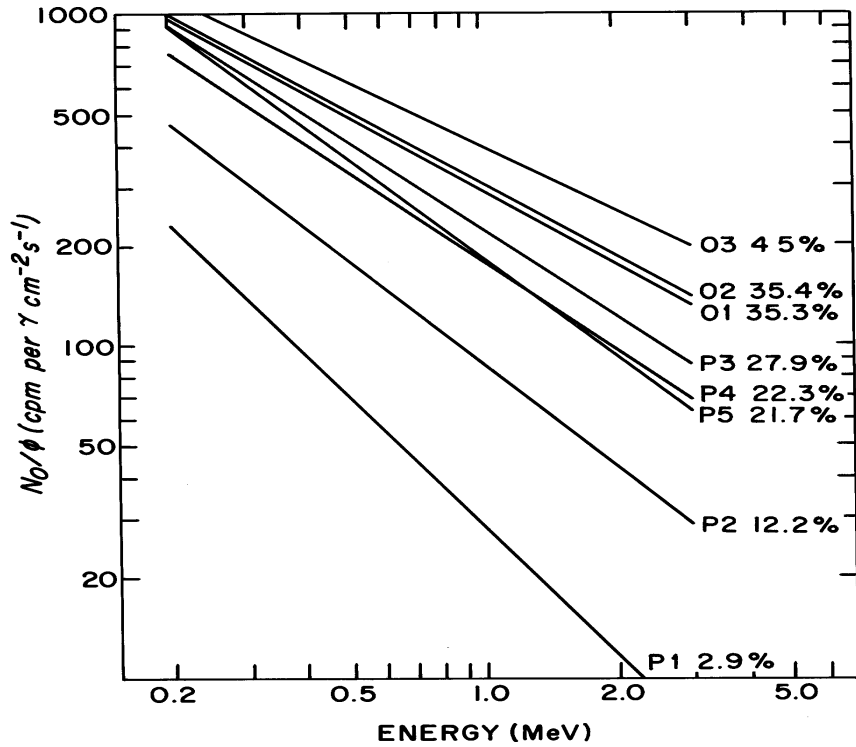


Figure 3.6. Count rate per unit incident flux at normal incidence ( $N_0/\phi$ ) as a function of energy for seven of the detectors listed in Table 3.1.

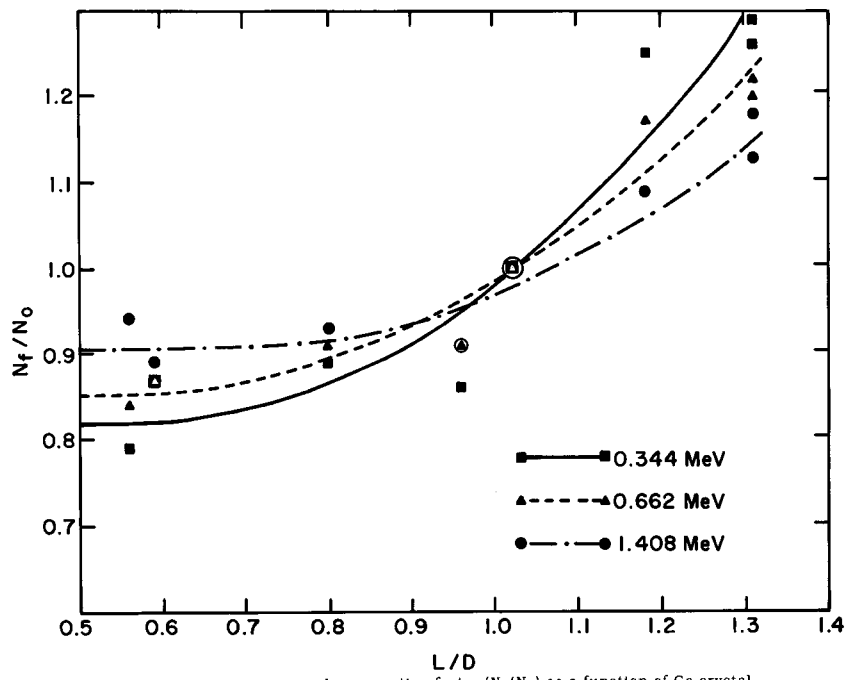


Figure 3.7. Angular correction factor ( $N_f/N_0$ ) as a function of Ge crystal length/diameter ( $L/D$ ) ratio at three different energies for a downward facing detector for a uniform with depth source profile in the soil.